Rethinking symbiotic metabolism: trophic strategies in the microbiomes of different sponge species

Burgsdorf I[1], Sizikov S[1], Squatrito V[1], Britstein M[1], Slaby BM[2], Cerrano C[3], Handley KM[4], Steindler L[1*]

[1]Department of Marine Biology, Leon H. Charney School of Marine Sciences, University of Haifa, Israel.

[2]GEOMAR Helmholtz Centre for Ocean Research Kiel, RD3 Marine Ecology, RU Marine Symbioses, Kiel, Germany.

[3]Department of Life and Environmental Sciences, Polytechnic University of Marche, Ancona, Italy.

[4]School of Biological Sciences, The University of Auckland, Auckland, New Zealand.

[*]**Corresponding author:** Laura Steindler

Department of Marine Biology, Leon H. Charney School of Marine Sciences

University of Haifa, 199 Aba Khoushy Ave

Mount Carmel, Haifa, 3498838, Israel

Phone: +972-4-8288987 / Fax: +972-4-8288267 / Email: lsteindler@univ.haifa.ac.il

Running title: Energy and carbon metabolism in sponge microbiomes

Abstract

In this study we describe the major lithoheterotrophic and autotrophic processes in 21 microbial sponge-associated phyla using novel and existing genomic and transcriptomic datasets. We show that a single gene family, molybdenum-binding subunit of dehydrogenase (*coxL*), likely evolved to benefit both lithoheterotrophic and organoheterotrophic symbionts, through adaptation to different inorganic and organic substrates. We show the main microbial carbon fixation pathways in sponges are restricted to specialized symbiotic lineages within five phyla. We also propose that sponge symbionts, in particular Acidobacteria, are capable of assimilating carbon through anaplerotic processes. However, the presence of symbionts genomically capable of autotrophy does not inform on their actual contribution to light and dark carbon fixation. Using radioisotope assays we identified variability in the relative contributions of chemosynthesis to total carbon fixation in different sponge species. Furthermore, the symbiosis of sponges with two closely related Cyanobacteria results in outcomes that are not predictable by analysis of *-omics* data alone: *Candidatus* Synechococcus spongiarum contributes to the holobiont carbon budget by transfer of photosynthates, while *Candidatus* Synechococcus feldmannii does not. Our results highlight the importance of combining sequencing data with physiology to gain a broader understanding of carbon metabolism within holobionts characterized by highly diverse microbiomes.

Introduction

Microbes can autotrophically assimilate inorganic carbon (Ci) via seven pathways including the Calvin-Benson-Bassham (CBB) cycle, the reductive tricarboxylic acid (rTCA) cycle, the Wood-Ljungdahl pathway (WL), and the 3-hydroxypropionate/4-hydroxybutyrate (3-HP/4-HB) cycle [1]. Additionally, various solo-acting enzymes can be involved in Ci assimilation without being part of *sensu stricto* carbon fixation. For instance, Ci assimilation in anaplerotic reactions was proposed to be abundant among marine planktonic heterotrophs [2–4]. Anaplerotic reactions undertaken by pyruvate (PYC) and phosphoenolpyruvate (PPC) carboxylases often occur at low levels to replace intermediates of the tricarboxylic acid (TCA) cycle. However, enhanced anaplerotic Ci assimilation was reported in marine planktonic lithoheterotrophs that combine organotrophy with the additional use of inorganic electron donors [4]. Malic enzyme (MEZ) was also shown to operate in the carboxylating (anaplerotic) direction, playing an essential role in the intracellular survival of the pathogen *Mycobacterium tuberculosis* [5, 6], in planktonic stages of *Pseudomonas aeruginosa* PAO1 [7] and in deep-sea Alphaproteobacteria [8].

Sponges (phylum Porifera) are ancient cosmopolitan filter-feeders [9, 10]. They play an important role in nutrient recycling by transforming Dissolved Organic Matter (DOM) into detrital Particulate Organic Matter, thereby making it available for other invertebrates in nutrient poor environments [11, 12]. Sponge-associated microbial communities include more than 60 bacterial and archaeal phyla [13], which are specific to their hosts [14–17]. These sponge-associated symbionts can be categorized based on their nutrition strategies, for instance (photo- and chemo-) autotrophic, organoheterotrophic and lithoheterotrophic. Heterotrophic symbionts can contribute up to 87% of the total sponge holobiont DOM assimilation [18], while autotrophic photosymbionts can contribute to host growth when exposed to light [19]. Beyond photosymbionts, various bacterial and archaeal

phyla in sponges harbor mechanisms associated with autotrophic metabolism, *e.g.*, the 3-HP/4-HB pathway in Thaumarchaeota, and the rTCA in Nitrospirota, Alphaproteobacteria and Oligoflexia [20–25]. However, carbon assimilation capacities within the sponge microbiome remain under-described, and the contribution of chemoautotrophy to the pool of microbially-fixed carbon in sponges has not yet been tested.

Net primary productivity and stable isotope analyses of the microbial and host sponge fractions showed that different species of symbiotic filamentous and unicellular Cyanobacteria differ in their ability to assimilate and transfer carbon to the host [26]. The unicellular *Parasynechococcus*-like cyanobacterial species are the most commonly reported in sponges [27, 28]. These include *Candidatus* Synechococcus spongiarum, enriched in 28 sponge species around the globe (including *Theonella swinhoei* from this study) [29], and *Candidatus* Synechococcus feldmannii, the symbiont of *Petrosia ficiformis* [30, 31]. The latter symbiosis is facultative, with *P. ficiformis* growing in light environments with *Ca.* S. feldmannii, and in dark-(cave)-environments without it. The heterotrophic microbial community of *P. ficiformis* is functionally and compositionally independent from the presence of *Ca*. S. feldmannii, being nearly identical in both structure and gene expression in specimens with and without this photosymbiont [31, 32]. This suggests that photosynthetically derived carbon may not be the main carbon source for heterotrophic *P. ficiformis*-associated symbionts. In this study we tested whether microbially fixed carbon or rather accumulation of DOM by the host represent the main supply of organic carbon to *P. ficiformis*.

Oxidation of diverse inorganic compounds, such as ammonia, nitrite, sulfide and thiosulfate, can serve as energy source for both autotrophic and lithoheterotrophic microorganisms, and these can also be found within the sponge microbiome [33–36]. Here, we characterized the dominant carbon fixation processes, and identified the energetic sources

used by lithoheterotrophs across different microbial species within sponge symbiotic communities. This was achieved through a genomic analysis of 402 symbiotic metagenome-assembled genomes (MAGs) from 10 different sponge species, and 39 metatranscriptomes from the sponge *P. ficiformis*. Further, using radioisotopes, we investigated the contribution of light and dark microbial carbon fixation in two sponge systems (*P. ficiformis* and *T. swinhoei*).

Materials and methods

Sponge sampling and microbial DNA purification

Three *P. ficiformis* specimens, 277c, 287ce, and 288c (c, cortex; e, endosome), were collected by SCUBA diving on January 6th, 2014, at depths 27, 23 and 15 meters, respectively, at Achziv nature marine reserve, Mediterranean Sea, Israel. Sponge samples were collected in compliance with permits from the Israel Nature and National Park Protection Authority. Microbial DNA was obtained as previously described [37]. Information about collection of additional nine sponge species can be found in Table S1.

Shotgun sequencing, assembly and binning

Preparation of metagenomic shotgun sequencing KAPA Hyper DNA libraries, sequencing, read trimming and *de novo* assemblies for the three *P. ficiformis* specimens were performed as previously described [37]. 50 genomes were binned using manual methods including visualization of differential coverage information derived from three *P. ficiformis* specimens (see File S1 at https://figshare.com/s/e305160ebd82d21bf151). DNA extraction, and assembly of MAGs from *T. swinhoei* (SP3), *Ircinia variabilis* (142) and *Aplysina aerophoba* (15L) are described in [38] and [21], respectively. Taxonomic affiliation of assembled scaffolds, binning of final MAGs, and relative abundance calculations are described in File S2.

121 ***MAG annotation and completeness estimation***

122 Open Reading Frames were identified using Prodigal v2.6.3 with the metagenome
123 options [39]. Protein sequences were queried against the Clusters of Orthologous Groups
124 (COGs) database (version 2014) as previously described (see File S3 at
125 https://figshare.com/s/786acca3672a820da570) [37]. The amino acid sequences were also
126 searched against the KEGG orthology (KO) database using standalone KofamKOALA 1.3.0
127 (see File S4 at https://figshare.com/s/a0ff9b495588b99e7c75) [40]. Selected enzymes were
128 annotated using previously published Hidden Markov models (HMM) [41] with individual
129 score thresholds (Table S2) using hmmsearch [42]. Phylogenomic tree construction and
130 taxonomic annotation was done using PhyloPhlAn2 [43]
131 (https://bitbucket.org/nsegata/phylophlan/wiki/phylophlan2), RAxML [44] as previously
132 described [45] and GTDB-Tk v1.3 with release r95 [46]. Trees were visualized using iTol
133 [47]. Completeness and contamination rates of all final MAGs were estimated with checkM
134 version 1.0.7 [48] using lineage_wf.

135 ***Annotation of transcriptomic data***

136 Metatranscriptomes were previously obtained from 39 *P. ficiformis* specimens
137 sampled in Ligurian Sea, Italy (as described in [31]), and quantified by Salmon software [49].
138 Translated sequences of the assembled and filtered bacterial metatranscriptomes were
139 assigned to the proteins of MAGs assembled from Israeli *P. ficiformis* specimen 277c using
140 blastp 2.2.30+ (*E*-value threshold = 1E−10, identity = 55%). Taxonomic annotation of
141 transcripts was determined based on the best hits (highest bit score and lowest *E*-value).
142 Transcripts with the same function and MAG affiliation were merged prior to analyses.
143 Expression of certain functions in a specific organism (MAG) was additionally confirmed
144 using mapping of the genes against metatranscriptome reads with bbmap tool v 37.62 [50]
145 (minimal identity=0.70, kmer size=13) from the BBtools package (https://jgi.doe.gov/data-

and-tools/bbtools/), (≥ 5 reads as a threshold). Functional annotation of the metatranscriptomes of *P. ficiformis* against the COG database was done as described previously [37] and search against the KEGG database was done via the GhostKOALA website using the genus_prokaryotes database (August 2020) [51]. Data was analyzed and visualized using the R packages dplyr, tidyr [http://tidyr.tidyverse.org], ggplot2 [52], plotly [53], reshape2 [54] and superheat [55]. A schematic representation of the bioinformatic analyses is available in Figure S1.

Carbon fixation measurements in Theonella swinhoei *and* Petrosia ficiformis *with* $H^{14}CO_3^-$

Photosynthetic (light) and chemosynthetic (dark) fixed carbon was measured in *P. ficiformis* (n=3) and *T. swinhoei* (n=4) specimens. For *P. ficiformis*, experiments were done on sponge cores, for *T. swinhoei*, on whole sponges and sponge cores. In *P. ficiformis* there are sponge areas facing light, that harbor Cyanobacteria (*Ca*. S. feldmannii), and others facing the shade, without Cyanobacteria. We thus used sponge cores from both areas with and without *Ca*. S. feldmannii in our experiments. Based on a pre-experiment on *T. swinhoei* cores, we determined the optimal incubation time of 2 hours (data not shown), used for all follow-up experiments. Next, we incubated cores (*P. ficiformis*) and whole sponges (*T. swinhoei*) in beakers with autoclaved seawater and 1 µl of $NaH^{14}CO_3$ (ARC, 150922, 1mCi/1ml) tracer for each 10 ml medium, stirring manually every 10 min. Beakers were exposed to light (100-150 and 50 µmol photons m^{-2} s^{-1}, for *P. ficiformis and T. swinhoei*, respectively) or to darkness. $NaH^{14}CO_3$ in the medium was measured every 30 min, by sampling 0.1 ml of seawater from each beaker and transferring to a scintillation vial containing 3 ml of scintillation fluid (UltimaGold®, Perkin-Elmer for *P. ficiformis* and Opti-fluor®, high flash-point LSC cocktail, Packard Bioscience for *T. swinhoei*). At the end of the incubation, each core section was left for 3 minutes on a paper towel to lose excess water,

weighted and then transferred to a vial containing 0.5 ml N,N-Dimethylformamide (Sigma), to release labeled fixed carbon from the tissue to the liquid, and 45 µl HCl 20% (Sigma), to release labeled/unlabeled non-fixed carbon. Sponge tissue was disintegrated manually with a plastic homogenizer and the vials were left uncovered for 48 hours in the chemical hood. After this time, 0.1 ml liquid was transferred to a new vial containing 3 ml scintillation fluid. All vials were measured in a liquid scintillation counter. Tri-Carb® 2810TR, Perkin Elmer and Tri-Carb® 1500, Lumitron, Packard Bioscience were used to measure the Discharges Per Min (DPM) for *P. ficiformis* and *T. swinhoei*, respectively. A detailed explanation about sponge sampling and core preparations for C fixation experiments is available in the File S2.

Results and Discussion

Overall, 47 bacterial and 3 archaeal MAGs belonging to 14 phyla were recovered from three *P. ficiformis* specimens, and are estimated to be 62 to 100% complete, with 0 to 5.5% contamination (Table S3). These genomes represent 38-41% of the assembled data and were investigated together with 8 additionally assembled MAGs from *T. swinhoei* (SP3), *Ircinia variabilis* (142) and *A. aerophoba* (15L) (Table S3), and additional 344 MAGs from previous studies [21, 24, 61–66, 25, 29, 37, 56–60] (Table S1) to identify all the dominant autotrophic and lithoheterotrophic processes found in sponge symbionts.

Autotrophy in sponge symbionts

We investigated the presence of known prokaryotic carbon fixation mechanisms among 402 sponge-associated MAGs derived from 10 sponge species (Figure 1, Figure S2, Tables S1, S3 and S4). The metabolic capacities of the sponge-associated symbionts are presented in Table S4 and their predicted trophic lifestyles, are summarized in Figure 2. Accordingly, we found that the autotrophic pathways 3-HP/4-HB, CBB and rTCA were

mainly restricted to Cyanobacteria, Tectomicrobia, Nitrospirota, and Thaumarchaeota phyla and two gammaproteobacterial orders.

RuBisCO-related genes were identified in all 16 cyanobacterial and 3 (out of 47) gammaproteobacterial genomes. Gammaproteobacterial MAGs from *P. ficiformis* lacked RuBisCO-related genes, or evidence of any other C-fixation pathways, and thus likely pursued a heterotrophic lifestyle. Yet, within these sponge species, 2 out of 5 gammaproteobacterial MAGs exhibited genomic potential for CO oxidation via carbon monoxide dehydrogenase (CODH), which can serve as energy source [67] . In *I. ramosa,* Gammaproteobacteria clades G2 (order UBA10353 and family LS-SOB) and G3 (order and family UBA4575) had genes for thiosulfate oxidation (Table S4), which can fuel carbon fixation (Figure 1, Figure S2) through RuBisCO (also found in three MAGs within G2 and G3 clades, File S2), indicating the potential for chemoautotrophy. Gammaproteobacteria G1, G4 and G5 did not have this pathway, yet encoded for CODH (*coxSML* and *coxG*) (Figure 1, Figure S2). Taken together, data show that gammaproteobacterial symbionts include two trophic groups: chemoautotrophs and lithoheterotrophs.

The filamentous Entotheonellia (phylum Tectomicrobia) found in the sponge *T. swinhoei* [61, 68, 69], were identified as chemoautotrophs based on the presence of a large cohort of CBB related genes [61]. We did not detect RuBisCO in the Tectomicrobia genomes (Table S4), which may be due to MAG incompleteness. Energy for carbon fixation in this phylum may be provided by oxidation of multiple inorganic donors, providing metabolic versatility to shifting environmental conditions within the host [70, 71]. Inorganic donors (and mechanisms for oxidation) include CO (CODH), H_2 (3b group hydrogenase), thiosulfate (Sox complex), and possibly even arsenite (AoxAB) (Table S4). Presence of arsenic was reported in sponges, at highest concentrations in *T. swinhoei* [72]. Oxidation of arsenite may have a dual function: energy source [73, 74], as well as detoxification of the highly toxic

arsenite to arsenate [75]. Calcium arsenate was in fact observed inside intracellular structures of filamentous Tectomicrobia [68]. Arsenite oxidation is not necessarily limited to filamentous Tectomicrobia, in fact we also found the arsenite oxidase genes (*aoxAB*) in Alphaproteobacteria, Chloroflexi, and Nitrospinota MAGs (Figure 1, Table S4).

The pyruvate synthase or pyruvate:ferredoxin oxidoreductase (PFOR, EC 1.2.7.1), which is required for the rTCA cycle, can also serve different non-autotrophic functions, such as energy production through fermentation of pyruvate to acetate. For example, sediment Chloroflexi harboring PFOR and acetyl-CoA synthetase [EC 6.2.1.1]) were predicted to biosynthesize ATP using this pathway [76]. Here, PFOR was identified in five Chloroflexi MAGs (from *A. aerophoba*, *P. ficiformis* and *I. ramosa*) that lack carbon fixation pathways and may serve an energy production role. Accordingly, a high abundance of acetyl-CoA synthetase (COG1042) was previously detected in diverse sponge microbial metagenomes [77]. We therefore hypothesize that in the studied sponges ATP production involving pyruvate conversion to acetyl-CoA (by PFOR), coupled with acetate formation (by acetyl-CoA synthetase), occurs in five specialized, sponge-associated Chloroflexi (Figure 1, Figure S2, Table S4).

Lithoheterotrophy and metabolism of inorganic compounds in sponge symbionts

We and others have detected genes for oxidation of diverse inorganic compounds, such as CO, nitrite, ammonia, and thiosulfate in the sponge microbial community [33–36]. Further, we reveal the potential for hydrogen oxidation, specifically by the Tectomicrobia derived from *T. swinhoei* and in a Bacteroidetes MAG from *P. ficiformis* (Figure 1, Table S4, Figure S2). Nitrogen processing by diverse members of the sponge microbiome has been analyzed in several studies (*e.g.*, [33, 36]). It was suggested that ammonia oxidation in sponges is uniquely performed by Thaumarchaeota [36]. Nitrite can be oxidized to nitrate by members of Nitrospirota, Alphaproteobacteria and Gammaproteobacteria symbionts [35]. We

speculate that oxidation of nitrite to nitrate may only be carried out by Nitrospirota, rather than also by Proteobacteria, as previously proposed [35]. We base this speculation on a stricter annotation of the genes involved (*nrxAB*) using both HMM profiles and KEGG annotations (File S2).

Orthologues of *amoABC/pmoABC* genes (involved in ammonia and/or methane oxidation [78, 79], Table S2) were here found also in Desulfobacterota (unclassified Deltaproteobacteria based on NCBI taxonomy), specifically in two MAGs deriving from *A. aerophoba* and *P. ficiformis* (Table S4, File S2). Based on sequence similarity, we predict that *amoABC/pmoABC* of Desulfobacterota are involved in methane oxidation (File S2). Besides methane to methanol oxidation (EC 1.14.18.3), these MAGs also have the potential to further oxidize methanol to formaldehyde (EC:1.1.2.10) (Table S4). Genomic potential for methane to formaldehyde oxidation was previously discovered in sponges, but was not affiliated with members of Desulfobacterota [36, 80]. *amoABC/pmoABC* subunits were shown to be also expressed within the sponge *P. ficiformis* (details provided below).

CO-oxidizing bacteria are lithoheterotrophs common in sponge microbiomes. Large (CoxL, COG1529) and middle (CoxM, COG1319) subunits of the molybdenum-rich aerobic form of CODH (Mo-CODH) are highly overrepresented in sponge-associated *versus* seawater microbial metagenomes [34]. Mo-CODH has been identified in gamma and alphaproteobacterial sponge symbionts [33, 34] and found to be expressed among phylogenetically diverse symbionts including Actinobacteria, Chloroflexi and Proteobacteria [81]. Yet the function of CoxL is variable, and its homologues are not solely responsible for CO oxidation. In fact, CoxL was shown to comprise two different forms (I and II), with form II (putative *coxL*) being involved in functions alternative to CO oxidation [67]. To establish the extent to which CO oxidation is abundant in sponge symbionts, determine potential alternative substrates beyond CO, and provide this information at a taxonomic level, we set

the following criteria: (i) genomic potential for CO oxidation was based on the presence of 4 subunits (*coxSMLG*) within MAGs, (ii) substrate specificity was based on clustering and reannotation of 2,406 translated *coxL* genes against the KO database and on reannotation of transcripts, (iii) taxonomy of transcripts was defined according to MAG-affiliation.

The Mo-CODH complex was found in 64% of all analyzed symbionts (Figure 1, Table S4), suggesting that CO oxidation is the most abundant process related to a lithoheterotrophic lifestyle in sponge symbionts. Overall, more than half of the protein sequences annotated as CoxL COG1529 belonged to Actinobacteria (29%) and Chloroflexi (22%), while Tectomicrobia and Actinobacteria had the highest average number of *coxL* genes (associated COG1529) per genome (Average = 29, SD = 5 and Average = 12, SD = 4, respectively) (Figure 3A). Among the two largest clusters, one is predicted to function as CO dehydrogenase (the mostly-orange cluster dominated by Actinobacteria, Figure 4), while the second large cluster could not be linked to any known function (the predominantly black cluster, where Chloroflexi prevail). Additional substrates for CoxL are likely isoquinaline (mostly violet cluster, dominated by Gammaproteobacteria) and nicotinate (green cluster, where Gemmatimonadetes and Chloroflexi prevail). Results therefore suggest that sponge symbionts can gain electrons from CO (lithoheterothrophs) and organic molecules (*e.g.*, isoquinaline and nicotinate; organoheterotrophs) via genes related to a large orthologous group - CoxL COG1529. Nevertheless, the substrate for more than half of the proteins annotated as CoxL COG1529 in sponge symbionts, remains unknown (black dots, Figure 4; N/A in Figure 3B).

While we showed here an extensive incidence of CODH within the sponge microbiome, some phyla were found to lack this functional capacity. Specifically, phyla with inherently autotrophic lifestyles (Cyanobacteria, Nitrospirota, and archaeal Thaumarchaeota) (Figure 2) and phyla specialized in the degradation of polysaccharide residues (Bacteroidota

295 [82, 83], Dadabacteria [84], and Verrucomicrobia [45, 85]), which did not contain CODH
296 (Figure 3B). An exception are the 2 out of 17 Poribacteria, also characterized as degraders of
297 diverse carbohydrate sources originating in the sponge matrix [36, 59, 86], which harbored
298 CODH (Clade P1 in Figure 1). However, CoxL in these two Poribacteria might function in
299 the oxidation of xanthin (see below), and they may thus not have a lithoheterotrophic
300 lifestyle. Mo-CODH should be distinguished from Nickel-CODH, which relates to the
301 anaerobic WL pathway. The latter was previously reported in sponge symbionts [21–23, 25],
302 but based on our analysis (combining KEGG, COG and HMM profiles annotations, Table
303 S2), we conclude that Nickel-CODH, and thus the WL pathway, is absent in the sponge
304 microbiome.

305 Taken together results indicate that the presence of CoxL COG1529 in sponge
306 symbionts can relate to both CO oxidation (as a part of CODH complex), and thus to a
307 lithoheterotrophic lifestyle, or the oxidation of different organic substrates. Similarly to other
308 symbiotic systems, including the human gut and legumes [67, 87], CO-oxidizing bacteria
309 appear to have an essential role in the sponge holobiont. The potential sources for CO in
310 sponges may include photoproduced CO derived from the ambient seawater [88, 89] and
311 biological hemoprotein degradation via heme oxygenase (HO) activity [67, 87, 90]. Genomic
312 potential for hemoprotein synthesis, transport and oxidation here found in specific members
313 of the sponge microbiome, and suggested as a potential CO source in sponges, is discussed in
314 File S2.

315 ***Gene expression of carbon fixation and energy production pathways: case study of* P.**
316 **ficiformis**

317 To study the activity of key processes related to carbon fixation and energy
318 production from oxidation of inorganic molecules, we conducted a genome-informed
319 metatranscriptomic analysis of the *P. ficiformis*-associated community. We linked 50 MAGs

(Table S3) with an assembled metatranscriptome dataset derived from 39 *P. ficiformis* specimens. 35% of transcripts aligned to protein sequences.

Our gene expression results confirm the results derived from the wider MAG analysis described above on the importance of CO oxidation in sponge symbionts, and further corroborate that specific sub-orthologs of COG1529 might provide symbionts with the ability to utilize alternative organic electron donors. The latter may be part of the DOC (or its residues) that is concentrated by the host's filtration activity [91]. Similar to other sponge species, results show CO-oxidizing bacteria were highly abundant in the sponge *P. ficiformis*, with more than half of the MAGs (64%, n=50) harboring CODH (Figure 1, Table S4), and with all MAGs affiliated to Actinobacteria (n=13), Acidobacteria (n=4), and Chloroflexi (n=9) harboring CODH. Here, we tested how the widespread genomic potential for CO oxidation relates to its expression across different symbiotic microbial phyla.

We confirmed the expression of CO dehydrogenase (K03520) among eight phyla including Acidobacteria, Actinobacteria, and Chloroflexi (Figure 5A). Acidobacteria and Chloroflexi expressed all four subunits of CODH, while Actinobacteria, Desulfobacterota, and Latescibacterota did not express the *coxG* subunit. The *coxG* gene was also absent from the form 1 (*bona fide* CO dehydrogenase) Mo-CODH from the chemoautotroph *Alkalilimnicola ehrlichei* MLHE-1 [67], suggesting that the presence of this gene is not crucial for CO oxidation [92, 93]. Interestingly, while the auxiliary subunits of CODH, affiliated to poribacterial MAGs, were expressed, the large CO-oxidizing subunit was absent in the representatives of this phylum. This may be explained by the functional annotation of the CODH complex as xanthine dehydrogenase (EC 1.17.1.4) in Poribacteria (Figures 3B, 5A and 6), suggesting that this phylum does not oxidize CO in sponges. Functional and taxonomic specialization for certain subgroups of COG1529 was also observed for additional members of the *P. ficiformis* symbiotic microbial community (Figure 5). For instance, a

suborthologous group annotated as a subunit of xanthine dehydrogenase (K13482) was exclusively linked to a single actinobacterial MAG (Actino_4, class *Acidimicrobiia*, order UBA5794, family SZUA-232), and a nicotinate dehydrogenase subunit (K18030) was linked to Gammaproteo_5 (order *Pseudomonadales*, family HTCC2089) (Figure 6).

It has been suggested that CODH supplies energy for enhanced anaplerotic reactions by pyruvate carboxylase (PYC) in planktonic marine Alphaproteobacteria [3]. Anaplerotic carbon assimilation may contribute differently to the actual biomass accumulation ranging 0.5–1.2% of the total carbon of cells [8] and 10-15% of protein [94] in different Alphaproteobacteria strains. Due to a high abundance of genes related to anaplerotic reactions (86%) within the fifty *P. ficiformis*-derived MAGs, we next determined the taxa that consistently expressed genes associated with anaplerotic carbon assimilation across multiple *P. ficiformis* specimens. Consistent expression by the same taxon across different specimens implies an enhanced anaplerotic flow, which can result in actual carbon assimilation due to relatively high carbon influx to the TCA cycle, while sporadic expression is more likely to be related to metabolic flexibility with periodical replenishment of TCA intermediates [4]. We observed prevalent expression (≥90% of all samples, n=39) of transcripts showing high similarity to anaplerotic proteins (PYC, malic enzyme [MEZ], and phosphoenolpyruvate carboxykinase [PCKA]) belonging to 3 Acidobacteria (order *Vicinamibacterales*), one Alphaproteobacteria (order UBA2966), and one Chloroflexi (order UBA3495). Thus, anaplerotic carbon assimilation in *P. ficiformis* might occur in Acidobacteria, Alphaproteobacteria and Chloroflexi. When genes were mapped against metatranscriptome reads, only the MAG-specific affiliation of *pckA* from Acidobacteria (MAG Acido_2) was confirmed (Figure 7). We further observed correlations between expression levels of *coxL* and PCKA transcripts, linked to Acido_2 MAGs, across twelve different *P. ficiformis* samples (Figure S3). In contrast to PYC, phosphoenolpyruvate

carboxylase (PPC) and MEZ, PCKA utilizes CO_2 rather than bicarbonate. We hypothesize that in Acido_2 within *P. ficiformis* and, possibly, in closely related *Vicinamibacterales* symbionts of *I. ramosa* (Figure 1, Figure S2, Clade Acd1), inorganic carbon assimilation may occur by CoxL supplying CO_2 to the anaplerotic reaction catalyzed by PCKA.

Genomic potential for CBB was here found in symbionts of the Cyanobacteria and Proteobacterota (Gammaproteobacteria) phyla and was previously reported for Tectomicrobia [61]. Here we investigated the expression of the large subunit of RuBisCO (*rbcL*) in *P. ficiformis.* As expected, all samples that harbored Cyanobacteria (pink phenotype [31], n=12) showed expression of *rbcL*. In addition, we observed expression of a gammaproteobacterial *rbcL* in 30 (out of 39) samples (Figure 5C). This suggests that the Italian population of *P. ficiformis* (used for the transcriptomics data) is associated with a specific gammaproteobacterial symbiont with CBB activity, providing capability for dark fixation, while the Israeli population of *P. ficiformis* (used for obtaining MAGs) appears to lack this symbiont. A biogeographic effect on the microbial composition of *P. ficiformis* was reported before [32, 38].

Microbial carbon fixation can also occur through the 3-HP/4-HB cycle, which was suggested to be energetically fueled by ammonia oxidation in sponge-associated archaea [36]. Thaumarchaeota MAGs from *P. ficiformis* harbored *amoABC* genes (Figure 1, Table S4) and expressed *amoC* (Figure S4), as well as acetyl-CoA/propionyl-CoA carboxylase, the key gene of the 3-HP/4-HB cycle (Figure 5C). These findings confirm the involvement of Thaumarchaeota in dark carbon fixation in this sponge species. Orthologues of *amoABC/pmoABC* were also found in Desulfobacterota from *P. ficiformis* and are attributed to methane oxidation as explained below. The *pmoA* subunit of this MAG was expressed in 37 out of the 39 *P. ficiformis* samples suggesting a wide distribution for methane oxidation in *P. ficiformis* (Figure S4A) .

395 ***Carbon fixation measurements in sponges***

396 Physiology experiments, using ^{14}C labelled bicarbonate can test the ability of
397 autotrophic carbon assimilation that is light dependent (photosynthetic activity) or that occurs
398 in darkness (dark primary production). Two sponge species were used in the ^{14}C labelled
399 bicarbonate fixation experiments: (1) *P. ficiformis*, harboring *Ca.* S. feldmannii, and (2) *T.*
400 *swinhoei*, with *Ca.* S. spongiarum. The latter sponge is also known to harbor a dense
401 population of filamentous Tectomicrobia that have genomic potential to fix carbon *via* CBB,
402 utilizing multiple inorganic energy sources (Table S4, Figure 1).

403 Light-mediated inorganic carbon fixation was detected in both species in the cortex
404 (external layer) of the sponge, where Cyanobacteria reside. While on average *ca*. 81-97% of
405 total (*i.e.* light+dark) carbon fixation occurred in light conditions in *P. ficiformis* (Figure 8B,
406 D), the overall contribution of light fixation in *T. swinhoei* ranged between 46 and 78%
407 (Figure 8A, C). Transfer of labelled photosynthates to internal sponge layers was only
408 observed for *T. swinhoei* (Figure 8A). In contrast, the labeled photosynthates produced by
409 *Ca*. S. feldmannii remained within the cortex of *P. ficiformis* (Figure 8B, D). The lack of
410 contribution of fixed organic carbon from *Ca*. S. feldmannii to internal layers of the sponge
411 host supports the previous hypothesis that the symbiotic role of this photosymbiont may not
412 be directly related to its photosynthetic properties, and rather to protection from solar
413 radiation via synthesis of pigments [31]. Accordingly, presence of a photosymbiont does not
414 directly imply transfer of organic carbon to its host, and alternative benefits need to be
415 investigated. Diverse trends in carbon contribution to the host were shown also for different
416 sponge species harboring *Ca.* S. spongiarum, and it was suggested that such variability may
417 relate to symbiont phylotypes (clades within *Ca.* S. spongiarum) [19, 26].

418 Chemosynthetic or dark carbon fixation in *T. swinhoei* represented 16.6-29.5% of
419 total fixation. Besides symbiotic Thaumarchaeota [38] and Nitrospirota [95], *T. swinhoei* is

also known to harbor abundant filamentous Tectomicrobia ('Entotheonella'). This symbiont may therefore be the main organism responsible for the observed dark-fixation in this sponge species, by means of CBB cycle, fueled by a wide range of inorganic energy sources.

In contrast to *T. swinhoei*, dark fixation provided a relatively low contribution to total fixation (0.1-4.5%) in *P. ficiformis*. This, despite that *P. ficiformis* harbors Nitrospirota [31] and Thaumarchaeota [31, 38] symbionts, phyla that we show here as capable of dark carbon fixation via the rTCA and 3-HP/4-HB cycles, respectively. Both cycles are energetically fueled by different stages of nitrification, with ammonia and nitrite oxidation processes driven by Thaumarchaeota and Nitrospirota, respectively. However, ammonia oxidation rates were shown to be ten times lower than nitrite oxidation rates in the Mediterranean sponges *Dysidea avara* and *Chondrosia reniformis* [96], suggesting a larger influence of the rTCA compared to the 3-HP/4-HB cycle towards dark carbon fixation. If a similar trend is relevant also to *P. ficiformis*, then Thaumarchaeota may contribute little fixed carbon, resulting in the very low dark fixation observed in the ^{14}C-label experiments. Nitrospirota were reported to have low relative abundance and activity in *P. ficiformis* [31], which can also explain their low impact to the overall carbon fixation in the holobiont. Finally, non-photosynthetic CBB fixation by Gammaproteobacteria, shown in this study for Italian *P. ficiformis* specimens based on detection of *rbcL* transcripts, may not be relevant in Israeli *P. ficiformis* specimens, where homologues of the same *rbcL* gene were not detected in metagenomes or MAGs (Figure 1, Figure S6). Taken together with the ^{14}C-label experiments conducted on Israeli *P. ficiformis* specimens, chemoautotrophic pathways have only a minor influence on the overall carbon fixation compared to the photoautotrophic activity of *Ca.* S. feldmannii.

A decreasing pattern in $H^{14}CO_3^-$ concentration in the medium in which the *P. ficiformis* cores were incubated was observed for both the Cyanobacteria-harboring cores (where $H^{14}CO_3^-$ was fixed by *Ca*. S. feldmannii) (Figure S5A, B), and the white cores without

Cyanobacteria (Figure S5A, C). Killed samples (formalin controls) did not show decreasing patterns of $H^{14}CO_3^-$ in the incubation medium (Figure S5), implying biologically active uptake in living cores in the dark as well as the light. Given the minimal dark fixation observed, we suggest that the uptake of $H^{14}CO_3^-$ by the sponge in the dark resulted from assimilation of bicarbonate via anaplerotic reactions followed by immediate respiration of most of the assimilated carbon to CO_2.

If the dark-fixed $H^{14}CO_3^-$ was indeed immediately respired back to CO_2, we should only have detected the decrease in labelled $H^{14}CO_3^-$ in the seawater if it had remained trapped inside the sponge tissue. We thus conducted an additional experiment with white (Cyanobacteria-free) *P. ficiformis* cores incubated with $H^{14}CO_3^-$ in the dark, and once the decrease of labelled $H^{14}CO_3^-$ in the medium was detected, we crushed the sponge tissue. This resulted in an increase of label in the medium indicating release of the labeled CO_2 from the sponge core back to the medium (Figure S5C). This supports a fast turnover of dark-fixed CO_2 in *P. ficiformis*, which might be related to anaplerotic carbon assimilation. Further, based on our results, anaplerotic carbon assimilation in *P. ficiformis* likely results in energy production rather than in biomass accumulation.

The anaplerotic rates in the laboratory conditions may be lower than in the natural environment, due to differences in accessibility to metabolically important compounds [97] such as electron donors (*e.g.*, pelagic CO). In fact, physiological experiments performed on planktonic Gammaproteobacteria showed increased rates of anaplerotic Ci assimilation when the appropriate energy source (*e.g.*, thiosulfate) and anaplerotic carbon acceptor (*e.g.*, pyruvate) were added [2]. We therefore cannot exclude that anaplerotic carbon assimilation in laboratory conditions might be different from the natural conditions.

Conclusions

We have shown that CO oxidation is ubiquitous in sponge symbionts, likely representing the main inorganic energy source for lithoheterotrophs. Different variations of CODH and *amoABC*/*pmoABC* found across symbiotic lineages have evolved towards oxidation of diverse inorganic (*e.g.*, CO and ammonia) and organic (*e.g.*, xanthine and methane) compounds, that may be dissolved in seawater, that is continuously pumped through the sponge water channels, or produced within the sponge holobiont. Anaerobic forms of CODH and the WL pathway, previously suggested as being part of the Ci-fixing metabolic repertoire of some sponge symbionts, were found to be absent from the sponge microbiome. Most sponge symbionts were found to be lithoheterotrophs or organoheterotrophs with the exception of taxonomically restricted groups of autotrophs that implement the 3-HP/4-HB, CBB, and rTCA pathways. We provide the first experimental evidence for dark fixation in sponges, particularly in *T. swinhoei*. We further suggest that dark fixation processes in *P. ficiformis* (and potentially other sponge species) may also involve anaplerotic carbon assimilation, which is likely carried out by Acidobacteria, and possibly also by Alphaproteobacteria and Chloroflexi. Finally, cyanobacterial *Parasynechococcus*-like symbionts were shown to be highly diverse in terms of their contribution to the overall holobiont carbon budget, with *Ca.* S. spongiarum sharing its photosynthates with the host, while *Ca.* S. feldmannii behaving as a 'selfish' guest.

Acknowledgments

The authors thank the Inter-University Institute (IUI) in Eilat, Israel, for their technical support in SCUBA dives and laboratory availability for physiology experiments. LS wishes to warmly thank Prof. Sven Beer and Prof. Micha Ilan for support with the experiments on *T. swinhoei*. Dr. Eyal Rahav and Dr. Natasha Belkin are thanked for advice on radioactive measurements and calculations. Dr. Stefan Green, director of the DNA

Services Facility at the University of Illinois at Chicago (UIC) is thanked for useful comments and suggestions on sequencing strategies. The authors also thank Igor Chebotar, high performance computing system (HPC) administrator of the faculty of natural sciences at University of Haifa for his technical support in software and hardware assistance.

Funding

This work was supported by funds provided by the Israel Science Foundation [Grant No. 1243/16] and by the Gordon and Betty Moore Foundation, through Grant GBMF9352.

Data availability

MAGs from this study can be found under NCBI bioprojects ID PRJNA515489 (*P. ficiformis*), PRJNA255756 (*T. swinhoei*), PRJNA712987 (*A. aerophoba*) and PRJNA273429 (*I. variabilis*).

Conflict of interest statement

The authors declare no conflict of interest.

References

1. Hügler M, Sievert SM. Beyond the Calvin cycle: autotrophic carbon fixation in the ocean. *Ann Rev Mar Sci* 2011; **3**: 261–289.

2. Sorokin DY. Oxidation of inorganic sulfur compounds by obligately organotrophic bacteria. *Microbiology* 2003; **72**: 641–653.

3. Moran MA, Buchan A, González JM, Heidelberg JF, Whitman WB, Klene RP, et al. Genome sequence of *Silicibacter pomeroyi* reveals adaptations to themarineenvironment. *Nature* 2004; **432**: 910–913.

4. Moran MA, Miller WL. Resourceful heterotrophs make the most of light in the coastal ocean. *Nat Rev Microbiol* 2007; **5**: 792–800.

5. Basu P, Sandhu N, Bhatt A, Singh A, Balhana R, Gobe I, et al. The anaplerotic node is essential for the intracellular survival of *Mycobacterium tuberculosis*. *J Biol Chem* 2018; **293**: 5695–5704.

6. Machová I, Snášel J, Zimmermann M, Laubitz D, Plocinski P, Oehlmann W, et al. *Mycobacterium tuberculosis* phosphoenolpyruvate carboxykinase is regulated by redox mechanisms and interaction with thioredoxin. *J Biol Chem* 2014; **289**: 13066–13078.

7. Wan N, Wang H, Ng CK, Mukherjee M, Ren D, Cao B, et al. Bacterial metabolism during biofilm growth investigated by13C tracing. *Front Microbiol* 2018; **9**: 1–9.

8. Tang K, Yang Y, Lin D, Li S, Zhou W, Han Y, et al. Genomic, physiologic, and proteomic insights into metabolic versatility in *Roseobacter* clade bacteria isolated from deep-sea water. *Sci Rep* 2016; **6**: 1–12.

9. Simion P, Philippe H, Baurain D, Jager M, Richter DJ, Di Franco A, et al. A Large and consistent phylogenomic dataset supports sponges as the sister group to all other animals. *Curr Biol* 2017; **27**: 958–967.

10. Feuda R, Dohrmann M, Pett W, Philippe H, Rota-Stabelli O, Lartillot N, et al. Improved modeling of compositional heterogeneity supports sponges as sister to all other animals. *Curr Biol* 2017; 1–7.

11. de Goeij JM, van Oevelen D, Vermeij MJ a, Osinga R, Middelburg JJ, de Goeij AFPM, et al. Surviving in a marine desert: the sponge loop retains resources within coral reefs. *Science* 2013; **342**: 108–10.

543 12. Maldonado M. Sponge waste that fuels marine oligotrophic food webs: a re-
544 assessment of its origin and nature. *Mar Ecol* 2016; **37**: 477–491.

545 13. Moitinho-Silva L, Nielsen S, Amir A, Gonzalez A, Ackermann GL, Cerrano C, et al.
546 The sponge microbiome project. *Gigascience* 2017; **6**: gix077.

547 14. Hentschel U, Hopke J, Horn M, Anja B, Wagner M, Hacker J, et al. Molecular
548 evidence for a uniform microbial community in sponges from different oceans
549 molecular evidence for a uniform microbial community in sponges from different
550 oceans. *Appl Environ Microbiol* 2002; **68**: 4431–4440.

551 15. Lafi FF, Fuerst J a., Fieseler L, Engels C, Goh WWL, Hentschel U. Widespread
552 distribution of Poribacteria in Demospongiae. *Appl Environ Microbiol* 2009; **75**:
553 5695–5699.

554 16. Taylor MW, Radax R, Steger D, Wagner M. Sponge-associated microorganisms:
555 evolution, ecology, and biotechnological potential. *Microbiol Mol Biol Rev* 2007; **71**:
556 295–347.

557 17. Webster NS, Taylor MW. Marine sponges and their microbial symbionts: love and
558 other relationships. *Environ Microbiol* 2012; **14**: 335–46.

559 18. Rix L, Ribes M, Coma R, Jahn MT, de Goeij JM, van Oevelen D, et al. Heterotrophy
560 in the earliest gut: a single-cell view of heterotrophic carbon and nitrogen assimilation
561 in sponge-microbe symbioses. *ISME J* 2020; 1751–7370.

562 19. Freeman CJ, Thacker RW. Complex interactions between marine sponges and their
563 symbiotic microbial communities. *Limnol Oceanogr* 2011; **56**: 1577–1586.

564 20. Botté ES, Nielsen S, Azmi M, Wahab A, Webster J, Robbins S, et al. Changes in the
565 metabolic potential of the sponge microbiome under ocean acidification. *Nat Commun*

2019; **10**: 2041–1723.

21. Bayer K, Jahn MT, Slaby BM, Moitinho-Silva L, Hentschel U. Marine sponges as *Chloroflexi* hot spots: Genomic insights and high-resolution visualization of an abundant and diverse symbiotic clade. *mSystems* 2018; **3**: e00150-18.

22. Astudillo-García C, Slaby BM, Waite DW, Bayer K, Hentschel U, Taylor MW. Phylogeny and genomics of SAUL, an enigmatic bacterial lineage frequently associated with marine sponges. *Environ Microbiol* 2018; **20**: 561–576.

23. Podell S, Blanton JM, Neu A, Agarwal V, Biggs JS, Moore BS, et al. Pangenomic comparison of globally distributed *Poribacteria* associated with sponge hosts and marine particles. *ISME J* 2019; **13**: 468–481.

24. Engelberts JP, Robbins SJ, Goeij JM De, Webster NS, Aranda M, Bell SC, et al. Characterization of a sponge microbiome using an integrative genome-centric approach. *ISME J* 2020.

25. Podell S, Blanton JM, Oliver A, Schorn MA, Agarwal V, Biggs JS, et al. A genomic view of trophic and metabolic diversity in clade-specific *Lamellodysidea* sponge microbiomes. *Microbiome* 2020; **8**: 2049–2618.

26. Freeman CJ, Thacker RW, Baker DM, Fogel ML. Quality or quantity: is nutrient transfer driven more by symbiont identity and productivity than by symbiont abundance? *ISME J* 2013; **7**: 1116–25.

27. Steindler L, Huchon D, Avni A, Ilan M. 16S rRNA phylogeny of sponge-associated Cyanobacteria. *Appl Environ Microbiol* 2005; **71**: 4127–4131.

28. Simister RL, Deines P, Botté ES, Webster NS, Taylor MW. Sponge-specific clusters revisited: A comprehensive phylogeny of sponge-associated microorganisms. *Environ*

Microbiol 2012; **14**: 517–524.

29. Burgsdorf I, Slaby BM, Handley KM, Haber M, Blom J, Marshall CW, et al. Lifestyle evolution in cyanobacterial symbionts of sponges. *MBio* 2015; **6**: e00391-15.

30. Usher KM, Fromont J, Sutton DC, Toze S. The biogeography and phylogeny of unicellular cyanobacterial symbionts in sponges from Australia and the Mediterranean. *Microb Ecol* 2004; **48**: 167–77.

31. Britstein M, Cerrano C, Burgsdorf I, Zoccarato L, Kenny N, Riesgo A, et al. Sponge microbiome stability during environmental acquisition of highly specific photosymbionts. *Environ Microbiol* 2020; **22**: 3593–3607.

32. Burgsdorf I, Erwin PM, Lopez-Legentil S, Cerrano C, Haber M, Frenk S, et al. Biogeography rather than association with Cyanobacteria structures symbiotic microbial communities in the marine sponge *Petrosia ficiformis*. *Front Microbiol* 2014; **5**: 529.

33. Taylor JA, Palladino G, Wemheuer B, Steinert G, Sipkema D, Williams TJ, et al. Phylogeny resolved, metabolism revealed: functional radiation within a widespread and divergent clade of sponge symbionts. *ISME J* 2020.

34. Thomas T, Rusch D, DeMaere MZ, Yung PY, Lewis M, Halpern A, et al. Functional genomic signatures of sponge bacteria reveal unique and shared features of symbiosis. *ISME J* 2010; **4**: 1557–1567.

35. Engelberts JP, Robbins SJ, de Goeij JM, Aranda M, Bell SC, Webster NS. Characterization of a sponge microbiome using an integrative genome-centric approach. *ISME J* 2020.

36. Robbins SJ, Song W, Engelberts JP, Glasl B, Slaby BM, Boyd J, et al. A genomic

612 view of the microbiome of coral reef demosponges. *ISME J* 2021.

613 37. Burgsdorf I, Handley KM, Bar-Shalom R, Erwin PM, Steindler L. Life at home and on
614 the roam: Genomic adaptions reflect the dual lifestyle of an intracellular, facultative
615 symbiont. *mSystems* 2019; **4**: e00057-19.

616 38. Haber M, Burgsdorf I, Handley KM, Rubin-Blum M, Steindler L. Genomic insights
617 into the lifestyles of Thaumarchaeota inside sponges. *Front Microbiol* 2021; **11**: 3441.

618 39. Hyatt D, Chen G-L, LoCascio PF, Land ML, Larimer FW, Hauser LJ. Prodigal:
619 prokaryotic gene recognition and translation initiation site identification. *BMC*
620 *Bioinformatics* 2010; **11**: 119.

621 40. Aramaki T, Blanc-Mathieu R, Endo H, Ohkubo K, Kanehisa M, Goto S, et al.
622 KofamKOALA: KEGG Ortholog assignment based on profile HMM and adaptive
623 score threshold. *Bioinformatics* 2020; **36**: 2251–2252.

624 41. Anantharaman K, Brown CT, Hug LA, Sharon I, Castelle CJ, Probst AJ, et al.
625 Thousands of microbial genomes shed light on interconnected biogeochemical
626 processes in an aquifer system. *Nat Commun* 2016; **7**: 13219.

627 42. Eddy SR. Profile hidden Markov models. *Bioinformatics* 1998; **14**: 755–763.

628 43. Segata N, Börnigen D, Morgan XC, Huttenhower C. PhyloPhlAn is a new method for
629 improved phylogenetic and taxonomic placement of microbes. *Nat Commun* 2013; **4**.

630 44. Stamatakis A. RAxML version 8: A tool for phylogenetic analysis and post-analysis of
631 large phylogenies. *Bioinformatics* 2014; **30**: 1312–1313.

632 45. Sizikov S, Burgsdorf I, Handley K, Lahyani M, Haber M, Steindler L. Characterization
633 of sponge□associated Verrucomicrobia: microcompartment□based sugar utilization
634 and enhanced toxin□antitoxin modules as features of host□associated *Opitutales*.

Environ Microbiol 2020; **22**: 4669–4688.

46. Parks DH, Chuvochina M, Waite DW, Rinke C, Skarshewski A, Chaumeil PA, et al. A standardized bacterial taxonomy based on genome phylogeny substantially revises the tree of life. *Nat Biotechnol* 2018; **36**: 996–1004.

47. Letunic I, Bork P. Interactive Tree Of Life (iTOL): An online tool for phylogenetic tree display and annotation. *Bioinformatics* 2006; **23**: 127–128.

48. Parks DH, Imelfort M, Skennerton CT, Hugenholtz P, Tyson GW. CheckM: assessing the quality of microbial genomes recovered from isolates, single cells, and metagenomes. *Cold Spring Harb Lab Press Method* 2015; **25**: 1043–1055.

49. Patro R, Duggal G, Love MI, Irizarry RA, Kingsford C. Salmon provides fast and bias-aware quantification of transcript expression. *Nat Methods* 2017; **14**: 417–419.

50. Bushnell B. BBMap□: A Fast , Accurate , Splice-Aware Aligner. *CA, USA Ernest Orlando Lawrence Berkeley Natl Lab Berkeley sourceforge.net/projects/bbmap/* 2014.

51. Kanehisa M, Sato Y, Morishima K. BlastKOALA and GhostKOALA: KEGG Tools for Functional Characterization of Genome and Metagenome Sequences. *J Mol Biol* 2016; **428**: 726–731.

52. Wickham H. ggplot2: Elegant Graphics for Data Analysis. 2016. Springer-Verlag New York.

53. Plotly Technologies Inc. Collaborative data science. 2015. Plotly Technologies Inc. Montréal, QC Date of publication.

54. Wickham H. Reshaping data with the reshape package. *J Stat Softw* 2007; **21**: 1–20.

55. Barter RL, Yu B. Superheat: An R package for creating beautiful and extendable

heatmaps for visualizing complex data. *J Comput Graph Stat* 2018; **27**: 910–922.

56. Astudillo-García C, Slaby BM, Waite DW, Bayer K, Hentschel U, Taylor MW. Phylogeny and genomics of SAUL, an enigmatic bacterial lineage frequently associated with marine sponges.

57. Britstein M, Devescovi G, Handley KM, Malik A, Haber M, Saurav K, et al. A new N -acyl homoserine lactone synthase in an uncultured symbiont of the red sea sponge *Theonella swinhoei*. *Appl Environ Microbiol* 2015; **82**: AEM.03111-15.

58. Gao Z, Wang Y, Tian R. Symbiotic adaptation drives genome streamlining of the cyanobacterial sponge symbiont '"*Candidatus* Synechococcus spongiarum"'. *MBio* 2014; **5**: e00079-14.

59. Kamke J, Rinke C, Schwientek P, Mavromatis K, Ivanova N, Sczyrba A, et al. The candidate phylum Poribacteria by single-cell genomics: New insights into phylogeny, cell-compartmentation, eukaryote-like repeat proteins, and other genomic features. *PLoS One* 2014; **9**: e87353.

60. Karimi E, Slaby BM, Soares AR, Blom J, Hentschel U, Costa R. Metagenomic binning reveals versatile nutrient cycling and distinct adaptive features in alphaproteobacterial symbionts of marine sponges. *FEMS Microbiol Ecol* 2018; **94**.

61. Liu F, Li J, Feng G, Li Z. New genomic insights into " *Entotheonella* " symbionts in *Theonella swinhoei*: Mixotrophy , anaerobic adaptation , resilience , and interaction. *Front Microbiol* 2016; **7**: 1333.

62. Liu F, Li J, Li Z. Draft genome sequence of "*Candidatus* Synechococcus spongiarum" m9, binned from a metagenome of South China Sea sponge *Theonella swinhoei*. *Genome Announc* 2017; **5**: e01307-16.

680 63. Slaby BM, Hackl T, Horn H, Bayer K, Hentschel U. Metagenomic binning of a marine
681 sponge microbiome reveals unity in defense but metabolic specialization. *Isme J* 2017;
682 **11**: 2465–2478.

683 64. Tian RM, Wang Y, Bougouffa S, Gao ZM, Cai L, Bajic V, et al. Genomic analysis
684 reveals versatile heterotrophic capacity of a potentially symbiotic sulfur-oxidizing
685 bacterium in sponge. *Environ Microbiol* 2014; **16**: 3548–3561.

686 65. Wilson MC, Mori T, Rückert C, Uria AR, Helf MJ, Takada K, et al. An environmental
687 bacterial taxon with a large and distinct metabolic repertoire. *Nature* 2014.

688 66. Gao Z-M, Zhou G-W, Huang H, Wang Y. The Cyanobacteria-dominated sponge
689 Dactylospongia elegans in the South China Sea: Prokaryotic community and
690 metagenomic insights. *Front Microbiol* 2017; **8**: 1387.

691 67. King GM, Weber CF. Distribution, diversity and ecology of aerobic CO-oxidizing
692 bacteria. *Nat Rev Microbiol* 2007; **5**: 107–118.

693 68. Keren R, Mayzel B, Lavy A, Polishchuk I, Levy D, Fakra SC, et al. Sponge-associated
694 bacteria mineralize arsenic and barium on intracellular vesicles. *Nat Commun* 2017; **8**:
695 1–12.

696 69. Haygood DJFMG. Identification of the antifungal peptide-containing symbiont of the
697 marine sponge *Theonella swinhoei* as a novel Gammaproteobacterium , '*Candidatus*
698 Entotheonella palauensis'. *Mar Biol* 2000; **136**: 969–977.

699 70. Richardson DJ. Bacterial respiration: a flexible process for a changing environment.
700 *Microbiology* 2000; **146 (Pt 3**: 551–571.

701 71. White DC, Sinclair PR. Branched electron-transport systems in Bacteria. In: Rose AH,
702 Wilkinson JF (eds).1971. Academic Press, pp 173–211.

703 72. Mayzel B, Aizenberg J, Ilan M. The elemental composition of demospongiae from the
704 Red Sea, Gulf of Aqaba. *PLoS One* 2014; **9**.

705 73. Santini JM, Vanden Hoven RN. Molybdenum-containing arsenite oxidase of the
706 chemolithoautotrophic arsenite oxidizer NT-26. *J Bacteriol* 2004; **186**: 1614–1619.

707 74. Branco R, Francisco R, Chung AP, Morais PV. Identification of an aox system that
708 requires cytochrome c in the highly arsenic-resistant bacterium *Ochrobactrum tritici*
709 SCII24. *Appl Environ Microbiol* 2009; **75**: 5141–5147.

710 75. Anderson GL, Williams J, Hille R. The purification and characterization of arsenite
711 oxidase from *Alcaligenes faecalis*, a molybdenum-containing hydroxylase. *J Biol*
712 *Chem* 1992; **267**: 23674–23682.

713 76. Hug L a, Castelle CJ, Wrighton KC, Thomas BC, Sharon I, Frischkorn KR, et al.
714 Community genomic analyses constrain the distribution of metabolic traits across the
715 Chloroflexi phylum and indicate roles in sediment carbon cycling. *Microbiome* 2013;
716 **1**: 22.

717 77. Fan L, Reynolds D, Liu M, Stark M, Kjelleberg S, Webster NS. Functional
718 equivalence and evolutionary convergence in complex communities of microbial
719 sponge symbionts. *Proc Natl Acad Sci U S A* 2012; **109**: E1878–E1887.

720 78. Bock E, Wagner M. Oxidation of Inorganic Nitrogen Compounds as an Energy
721 Source. In: Rosenberg E, DeLong EF, Lory S, Stackebrandt E, Thompson F (eds). *The*
722 *Prokaryotes: Prokaryotic Physiology and Biochemistry*. 2013. Springer Berlin
723 Heidelberg, Berlin, Heidelberg, pp 83–118.

724 79. Lontoh S, DiSpirito AA, Krema CL, Whittaker MR, Hooper AB, Semrau JD.
725 Differential inhibition in vivo of ammonia monooxygenase, soluble methane

monooxygenase and membrane-associated methane monoxygenase by phenylacetylene. *Environ Microbiol* 2000; **2**: 485–494.

80. Glasl B, Robbins S, Frade PR, Marangon E, Laffy PW, Bourne DG, et al. Comparative genome-centric analysis reveals seasonal variation in the function of coral reef microbiomes. *ISME J* 2020; **14**: 1435–1450.

81. Feng G, Zhang F, Banakar S, Karlep L, Li Z. Analysis of functional gene transcripts suggests active CO2 assimilation and CO oxidation by diverse bacteria in marine sponges. *FEMS Microbiol Ecol* 2019; **95**.

82. Rajilić-Stojanović M, de Vos WM. The first 1000 cultured species of the human gastrointestinal microbiota. *FEMS Microbiol Rev* 2014; **38**: 996–1047.

83. Grondin JM, Tamura K, Déjean G, Abbott DW, Brumer H. Polysaccharide utilization loci: Fueling microbial communities. *J Bacteriol* 2017; **199**: 1–15.

84. Graham ED, Tully BJ. Marine Dadabacteria exhibit genome streamlining and phototrophy-driven niche partitioning. *ISME J* 2020.

85. Sichert A, Corzett CH, Schechter MS, Unfried F, Markert S, Becher D, et al. *Verrucomicrobia* use hundreds of enzymes to digest the algal polysaccharide fucoidan. *Nat Microbiol* 2020.

86. Jahn MT, Markert SM, Ryu T, Ravasi T, Stigloher C, Hentschel U, et al. Shedding light on cell compartmentation in the candidate phylum *Poribacteria* by high resolution visualisation and transcriptional profiling. *Sci Rep* 2016; **6**: 35860.

87. Hopper CP, De La Cruz LK, Lyles K V., Wareham LK, Gilbert JA, Eichenbaum Z, et al. Role of carbon monoxide in host–gut microbiome communication. *Chem Rev* 2020.

88. Stubbins A, Hubbard V, Uher G, Law CS, Upstill-Goddard RC, Aiken GR, et al.

749 Relating carbon monoxide photoproduction to dissolved organic matter functionality.
750 *Environ Sci Technol* 2008; **42**: 3271–3276.

751 89. Zuo Y, Jones RD. Formation of carbon monoxide by photolysis of dissolved marine
752 organic material and its significance in the carbon cycling of the oceans.
753 *Naturwissenschaften* 1995; **82**: 472–274.

754 90. King GM, Crosby H. Impacts of plant roots on soil CO cycling and soil-atmosphere
755 CO exchange. *Glob Chang Biol* 2002; **8**: 1085–1093.

756 91. Pita L, Rix L, Slaby BM, Franke A, Hentschel U. The sponge holobiont in a changing
757 ocean: from microbes to ecosystems. *Microbiome* 2018; **6**: 46.

758 92. Gourlay C, Nielsen DJ, Evans DJ, White JM, Young CG. Models for aerobic carbon
759 monoxide dehydrogenase: Synthesis, characterization and reactivity of paramagnetic
760 MoVO(μ-S)CuI complexes. *Chem Sci* 2018; **9**: 876–888.

761 93. Wilcoxen J, Zhang B, Hille R. The Reaction of the molybdenum- and copper-
762 containing carbon monoxide dehydrogenase from *Oligotropha carboxydovorans* with
763 quinones. *Biochemistry* 2011; **50**: 1910–1916.

764 94. Tang KH, Feng X, Tang YJ, Blankenship RE. Carbohydrate metabolism and carbon
765 fixation in *Roseobacter denitrificans* OCh114. *PLoS One* 2009; **4**.

766 95. Schmitt S, Tsai P, Bell J, Fromont J, Ilan M, Lindquist N, et al. Assessing the complex
767 sponge microbiota: core, variable and species-specific bacterial communities in marine
768 sponges. *ISME J* 2012; **6**: 564–76.

769 96. Schläppy ML, Schöttner SI, Lavik G, Kuypers MMM, de Beer D, Hoffmann F.
770 Evidence of nitrification and denitrification in high and low microbial abundance
771 sponges. *Mar Biol* 2010; **157**: 593–602.

772 97. Hesselsoe M, Nielsen JL, Roslev P, Nielsen PH. Isotope labeling and
773 microautoradiography of active heterotrophic bacteria on the basis of assimilation of
774 14CO2. *Appl Environ Microbiol* 2005; **71**: 646–655.

775

776 **Figure legends**

777 **Figure 1**. **Phylogenomic tree showing the distribution and diversity of carbon
778 assimilation and energy production pathways across microbial symbiont taxonomy and
779 host species**. The phylogenomic tree (N=399 MAGs) was constructed based on concatenated
780 universal markers (PhyloPhlAn2). Labels marked with a hollow star are MAGs assembled in
781 this study from the *P. ficiformis* specimen 277c. Labels marked with a colored star are eight
782 MAGs assembled from the *A. aerophoba* specimen 15, *T. swinhoei* specimen SP3 and *I.
783 variabilis* specimen 142. The tree is rooted to the Archaea group. Figure S6 represents an
784 enhanced version (MAGs names are displayed) of this tree. Acd1, class Vicinamibacteria,
785 order *Vicinamibacterales*, family UBA8438. C1, order *Cyanobacteriales*, family
786 *Desertifilaceae*. C2, order *Synechococcales*, family *Cyanobiaceae*. CHL1, class
787 Dehalococcoidia, order UBA3495. CHL2, class Anaerolineae, order SBR1031. G1, order
788 GCA-2729495. G2, order UBA10353, family LS-SOB. G3 (single MAG), order UBA4575.
789 G4, order *Pseudomonadales*, *Pseudohongiellaceae* family. G5, order *Pseudomonadales*,
790 HTCC2089 family. P1, class and order WGA-4E, unknown family. S1, unknown class. S2,
791 UBA2968 class and order. Poribacteria_ADFK02.1_Kamke_2014,
792 Poribacteria_AQPC01.1_Kamke_2014 and Poribacteria_ASZM01.1_Kamke_2014 were
793 excluded from the phylogenomic tree due to incomplete marker genes set.

794 *CO is not always a target molecule for the *coxSMLG* complex as it was shown here
795 for *Poribacteria*.

796

Figure 2. Predicted lifestyle for different taxonomic groups (Phylum/Class) of sponge symbionts. Heat map represents percentage of genomes with predicted lifestyle, text represents number of MAGs. The colors of the MAGs correspond to the most abundant lifestyle: lithoheterotrophs (red), autotrophs implementing CBB (green) and other chemoautotrophs (violet). The relevant functions can be found in Table S4. Here, heterotroph means organoheterotroph. AR, anaplerotic reaction.

*MAGs of Tectomicrobia (Entotheonellia) class possess incomplete genomic potential for utilization of CBB pathways.

Figure 3. Functional diversity and distribution of COG1529 orthologs across symbiotic bacterial phyla. (A) Number of proteins annotated as COG1529 per genome in different taxonomic groups (Phylum/Class) of sponge symbionts. (B) Functional diversity of the COG1529 orthologous group. Heat map represents percentages of genes with various functions (KEGG annotation) for different taxonomic groups (Phylum/Class) of sponge symbionts. Text represents number of sequences. Percentages of CO-oxidizing *coxL* (K03520) out of total COG1529 are presented on the right. K03520, CO; K07303, isoquinoline; K11177, xanthine; K18030, nicotinate; K16877, 2-furoyl-CoA; K07469, aldehyde; K12528, selenate; K11178, xanthine; K03518, CO; K09386, CO (KO annotation, target molecule).

Figure 4. Taxonomic affiliation and hypothesized substrate for CoxL (COG1529) across diversity of sponge-associated MAGs (N=402). Visualization of sequence-based clustering of 2406 proteins annotated as COG1529. Size of the dots is proportional to the length of the protein (in the range of 35-1250 amino acids, average = 682, SD = 207 amino acids). 720 out of 867 sequences forming the largest group (the predominantly black cluster)

have unknown function. 674 out of 784 sequences forming the second largest group (the predominantly orange cluster) were annotated as Mo-binding subunit of the CO dehydrogenase (K03520).

Figure 5. Expression of carbon assimilation and CO oxidation-related functions in the different phyla of *P. ficiformis* symbionts. The analyses are based on cumulative binary (1 – expressed, 0 – not expressed) expression of transcripts (N=39 transcriptomes). Transcripts with the same function and MAG affiliations are merged. (A) the four subunits of CODH (subunits with the same taxonomy are connected by lines), (B) anaplerotic fixation, and (C) carbon assimilation genes. Taxonomy of transcripts was assigned if the transcript was linked to the gene of the assembled MAG. Larger dots represent proportion of expression across samples for a certain taxonomy group (Phylum/Class). Transcripts with not assigned (NA) taxonomy (not linked to any assembled MAG) are given as black dots representing mean values (A) or violin plots representing overall distribution of transcripts (B and C). Genes: *mez*, malic enzyme; *pckA*, phosphoenolpyruvate carboxykinase; *ppc*, phosphoenolpyruvate carboxylase; *pyc*, pyruvate carboxylasev *accA*, subunit of acetyl-CoA carboxylase; *hyuA*, subunit of acetone carboxylase; *porA*, subunit of pyruvate synthase (PFOR); *rbcL*, large subunit of RuBisCO.

Figure 6. Expression of COG1529 and the variety of its hypothesized target molecules across phyla/classes of sponge symbionts in *P. ficiformis*. The analyses are based on cumulative binary (1 – expressed, 0 – not expressed) expression of transcripts with the same function and taxonomy (transcripts with the same KEGG annotations and MAG affiliations are merged) related to the different transcripts annotated as COG1529 across 39 samples of *P. ficiformis*. Taxonomy of transcripts is assigned if the transcript was linked to

847 the gene of the assembled MAG. The potential target molecule is written in brackets. Larger
848 dots represent proportion of expression across samples (average values from the binary data)
849 for a certain taxonomy group (Phylum/Class). Violin plots (B and C) represent distribution of
850 transcripts with no assigned taxonomy (NA).
851
852 **Figure 7. Anaplerotic carbon assimilation in *P. ficiformis* based on gene**
853 **expression data (N=39).** Cumulative binary expressions of transcripts related to anaplerotic
854 carbon assimilation with identical functional (in bracket) and species (linked to a certain
855 MAG) affiliations. Larger dots represent proportion of expression across samples. Genes that
856 showed prevalent expression (>90% of samples) and their prevalence were also confirmed by
857 direct mapping against the metatranscriptome reads (>90% of samples) are marked in red.
858 MEZ, malic enzyme; PCKA, phosphoenolpyruvate carboxykinase; PPC,
859 phosphoenolpyruvate carboxylase; PYC, pyruvate carboxylase.
860
861 **Figure 8. Light and dark carbon fixation in *T. swinhoei* (left insert) and *P.**
862 ***ficiformis* (right insert).** In inserts, circles schematically represent cores with numbers of
863 replications. Amounts (µg/g) of fixed labeled Ci across parallel sections of the sponge,
864 including the most external (outer 2 mm, harboring cyanobacterial symbionts) and internal
865 (cyanobacteria-free) sections. (A and C) Two specimens of *T. swinhoei* were used for each
866 experiment, one was incubated in light and one in dark for two hours. At the end of the
867 incubation, cylinders were cut out of the sponge and divided into 6-7 sections to establish
868 labeled carbon fixation. Mean ± SD (n= 9 (A), and n= 7 (C) for light and n=10 (A), and n= 8
869 (C) dark conditions). CaSs, *Ca*. S. spongiarum. (B and D) Cores derived from light
870 (cyanobacteria harboring) and dark (cyanobacteria-free) exposed parts of one specimen of *P.*
871 *ficiformis* for each experiment were incubated for two hours with $H^{14}CO_3^-$, cores were then

872 cut and divided into 3 sections to establish labeled carbon fixation. Mean ± SD (n=4 for light

873 and n=4 for dark conditions). CaSf, *Ca*. S. feldmannii.

Tree scale: 1

bootstrap

- 65
- 73.75
- 82.5
- 91.25
- 100

Phylum / Class (colored ranges)

- Thaumarchaeota
- Deinococcota
- Dadabacteria
- Patescibacteria
- Actinobacteria
- Chloroflexi
- Nitrospinota
- Spirochaetota
- Bdellovibrionota
- Poribacteria
- Latescibacterota
- Acidobacteria
- Bacteroidota
- Gemmatimonadota
- Nitrospirota
- Myxococcota
- Desulfobacterota
- Tectomicrobia
- Verrucomicrobia
- Cyanobacteria
- Alphaproteobacteria
- Gammaproteobacteria

Sponge species (color strips)

- *Aplysina aerophoba*
- *Carteriospongia foliascens*
- *Dactylospongia elegans*
- *Haliclona cymaeformis*
- *Ircinia ramosa*
- *Ircinia variabilis*
- *Lamellodysidea herbacea*
- *Petrosia ficiformis*
- *Spongia officinalis*
- *Theonella swinhoei*

Oxidation

- CO* (*coxSMLG*)
- Sulfur-related compounds
- Nitrogen-related compounds
- Arsenite
- H_2

Carbon assimilation and related

- PYC/PPC
- PEPCK
- MEZ
- Acetone carboxylase
- CBB cycle
- rTCA
- Partial genomic potential for CBB and PFOR
- Fermentation to acetate
- Acetyl-CoA carboxylase
- Glyoxylate cycle
- 3-HP/4-HB

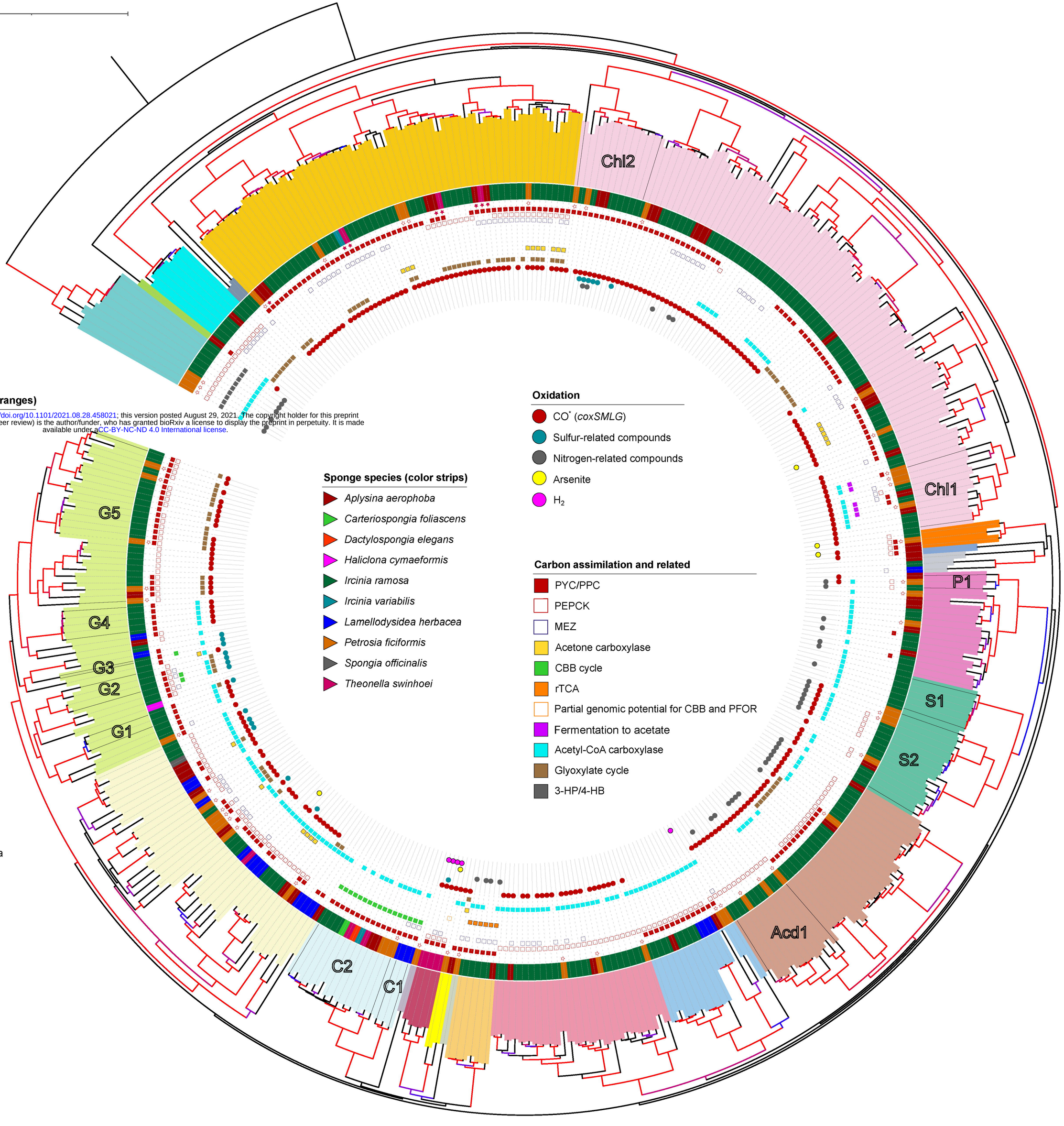

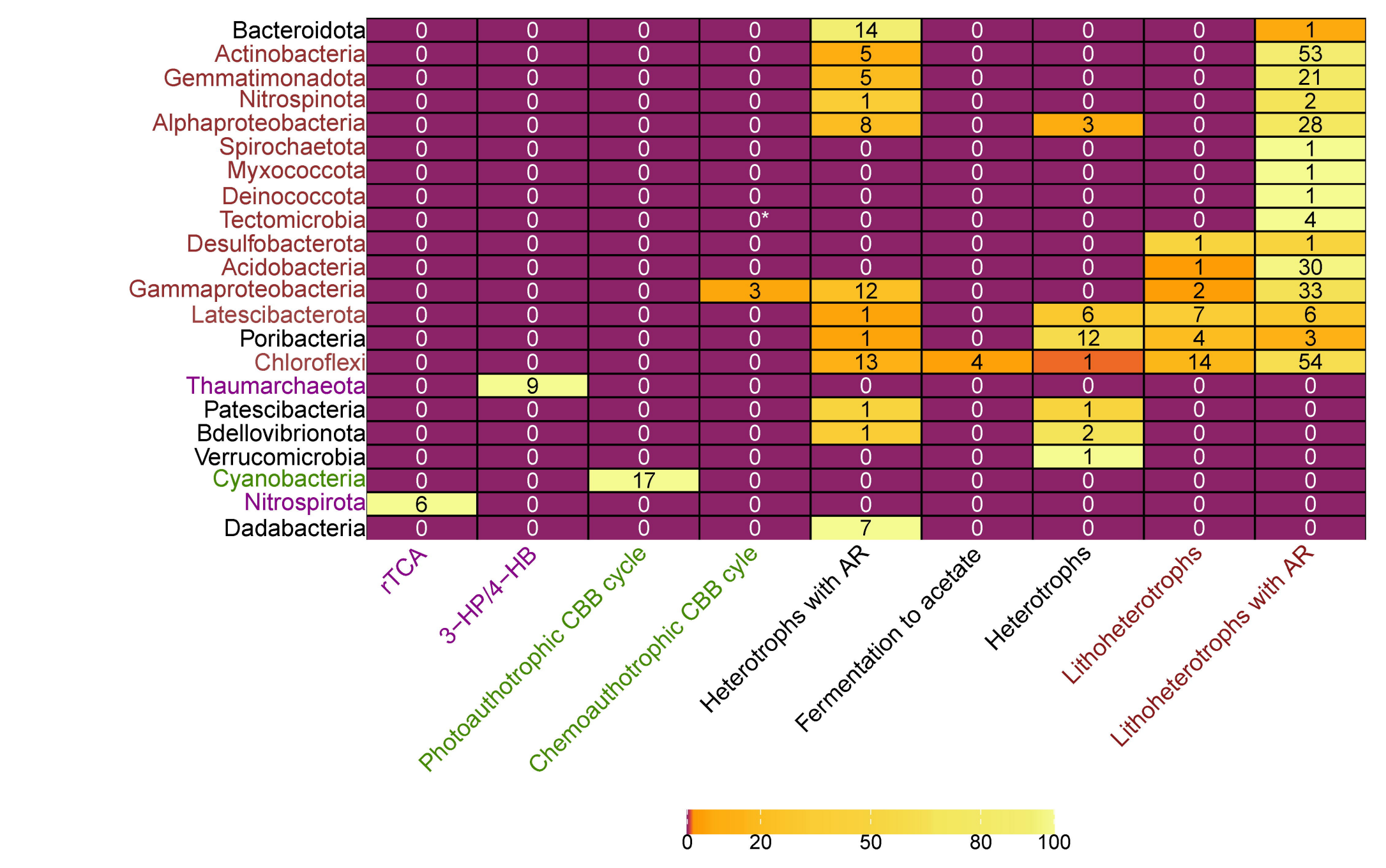
Bacteroidota 0 0 0 0 14 0 0 0 1
Actinobacteria 0 0 0 0 5 0 0 0 53
Gemmatimonadota 0 0 0 0 5 0 0 0 21
Nitrospinota 0 0 0 0 1 0 0 0 2
Alphaproteobacteria 0 0 0 0 8 0 3 0 28
Spirochaetota 0 0 0 0 0 0 0 0 1
Myxococcota 0 0 0 0 0 0 0 0 1
Deinococcota 0 0 0 0 0 0 0 0 1
Tectomicrobia 0 0 0 0* 0 0 0 0 4
Desulfobacterota 0 0 0 0 0 0 0 1 1
Acidobacteria 0 0 0 0 0 0 0 1 30
Gammaproteobacteria 0 0 0 3 12 0 0 2 33
Latescibacterota 0 0 0 0 1 0 6 7 6
Poribacteria 0 0 0 0 1 0 12 4 3
Chloroflexi 0 0 0 0 13 4 1 14 54
Thaumarchaeota 0 9 0 0 0 0 0 0 0
Patescibacteria 0 0 0 0 1 0 1 0 0
Bdellovibrionota 0 0 0 0 1 0 2 0 0
Verrucomicrobia 0 0 0 0 0 0 1 0 0
Cyanobacteria 0 0 17 0 0 0 0 0 0
Nitrospirota 6 0 0 0 0 0 0 0 0
Dadabacteria 0 0 0 0 7 0 0 0 0
rTCA
3−HP/4−HB
Photoauthotrophic CBB cycle
Chemoauthotrophic CBB cyle
Heterotrophs with AR
Fermentation to acetate
Heterotrophs
Lithoheterotrophs
Lithoheterotrophs with AR
0
20
50
80
100

A

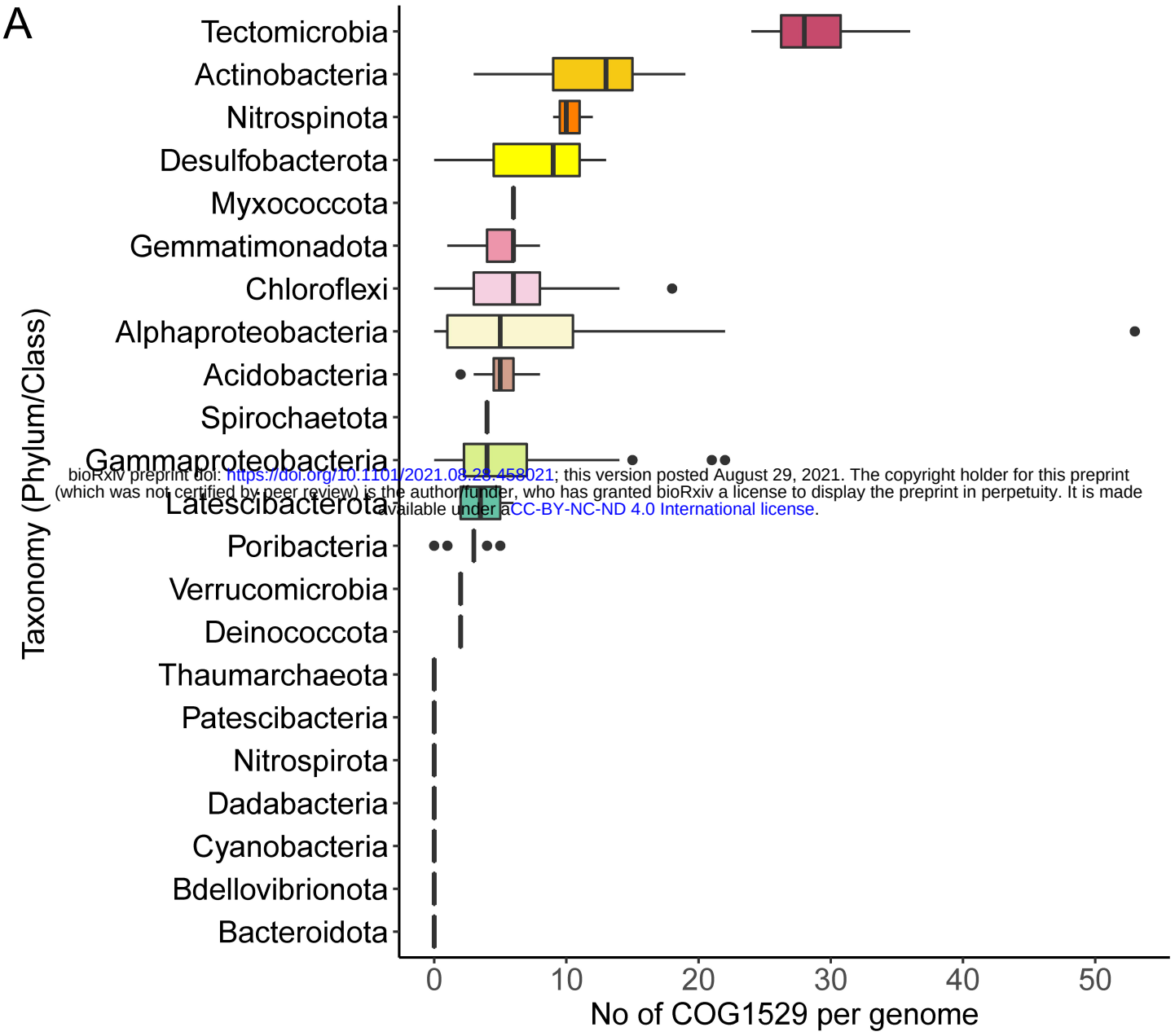

B

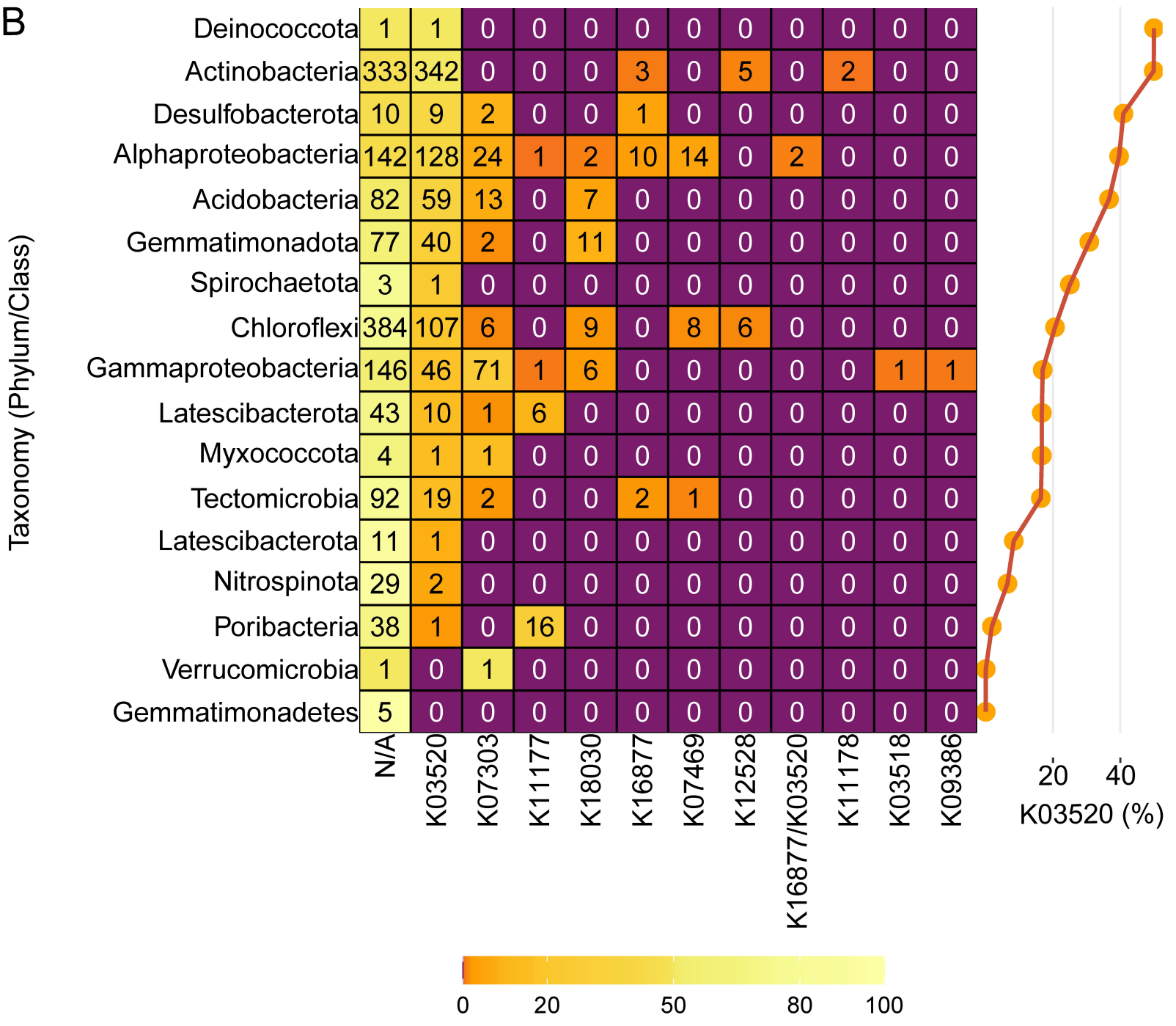

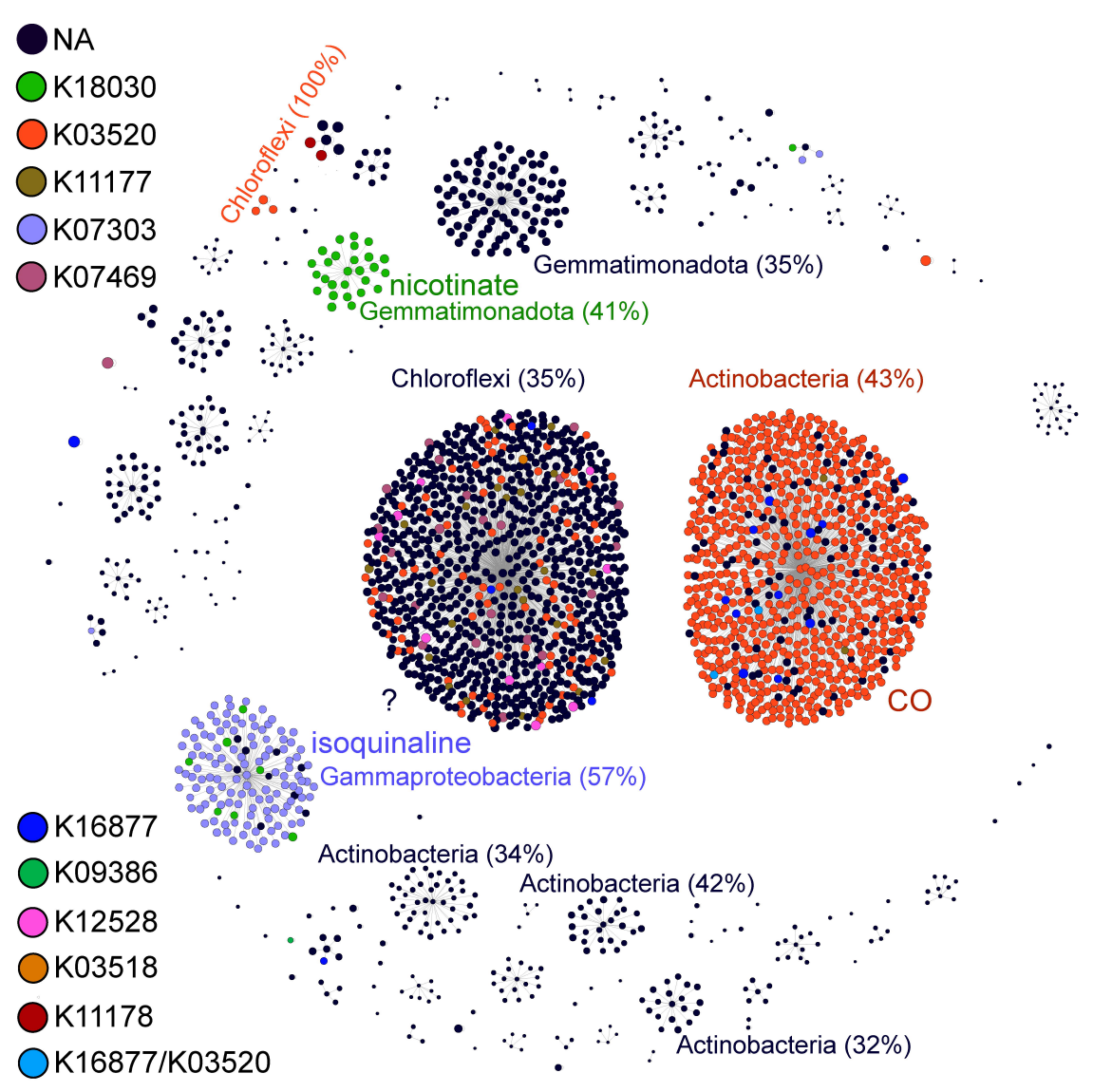
NA
K18030
K03520
K11177
K07303
K07469
Chloroflexi (100%)
Gemmatimonadota (35%)
nicotinate
Gemmatimonadota (41%)
Chloroflexi (35%)
Actinobacteria (43%)
?
CO
isoquinaline
Gammaproteobacteria (57%)
K16877
K09386
K12528
K03518
K11178
K16877/K03520
Actinobacteria (34%)
Actinobacteria (42%)
Actinobacteria (32%)

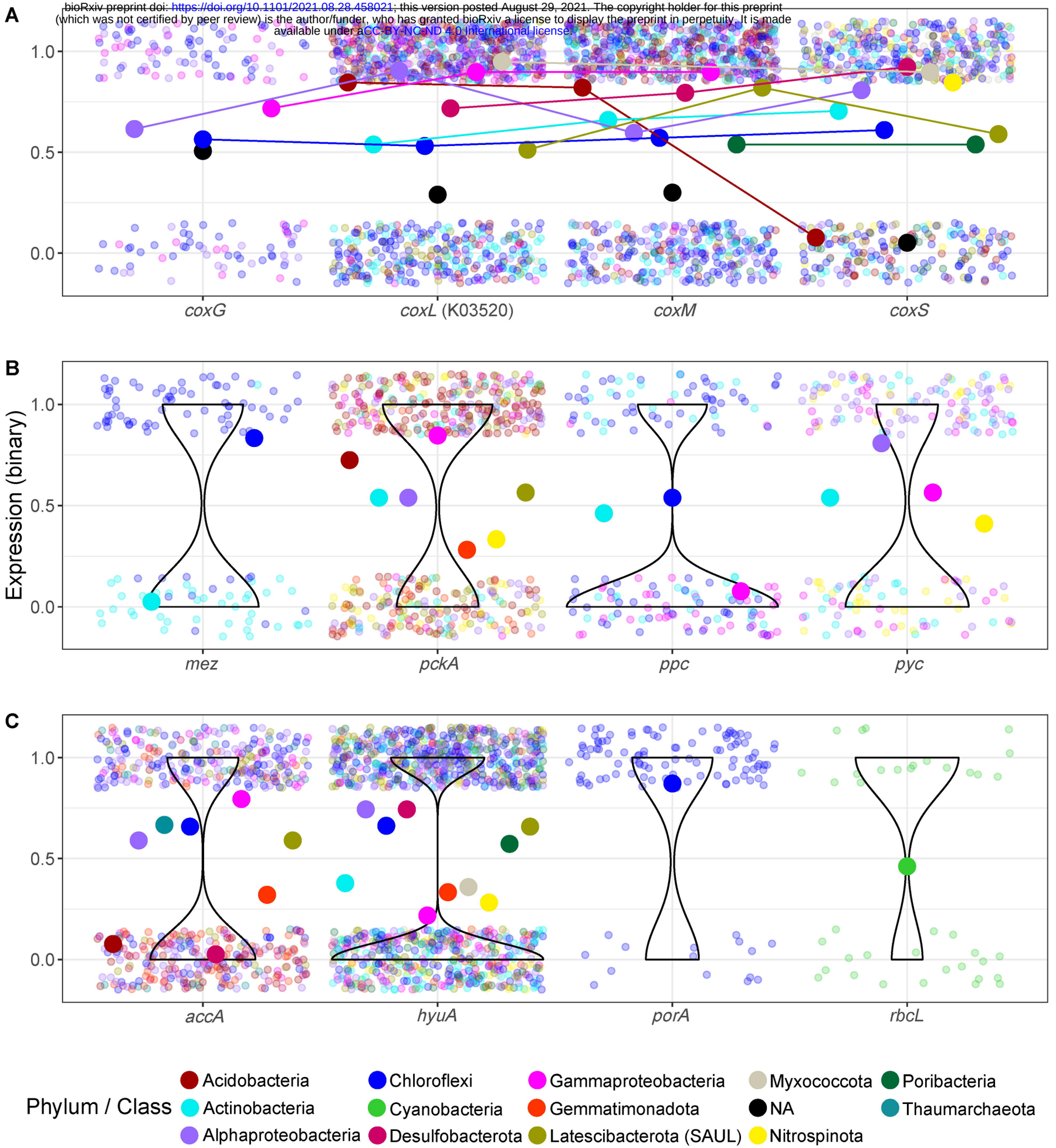

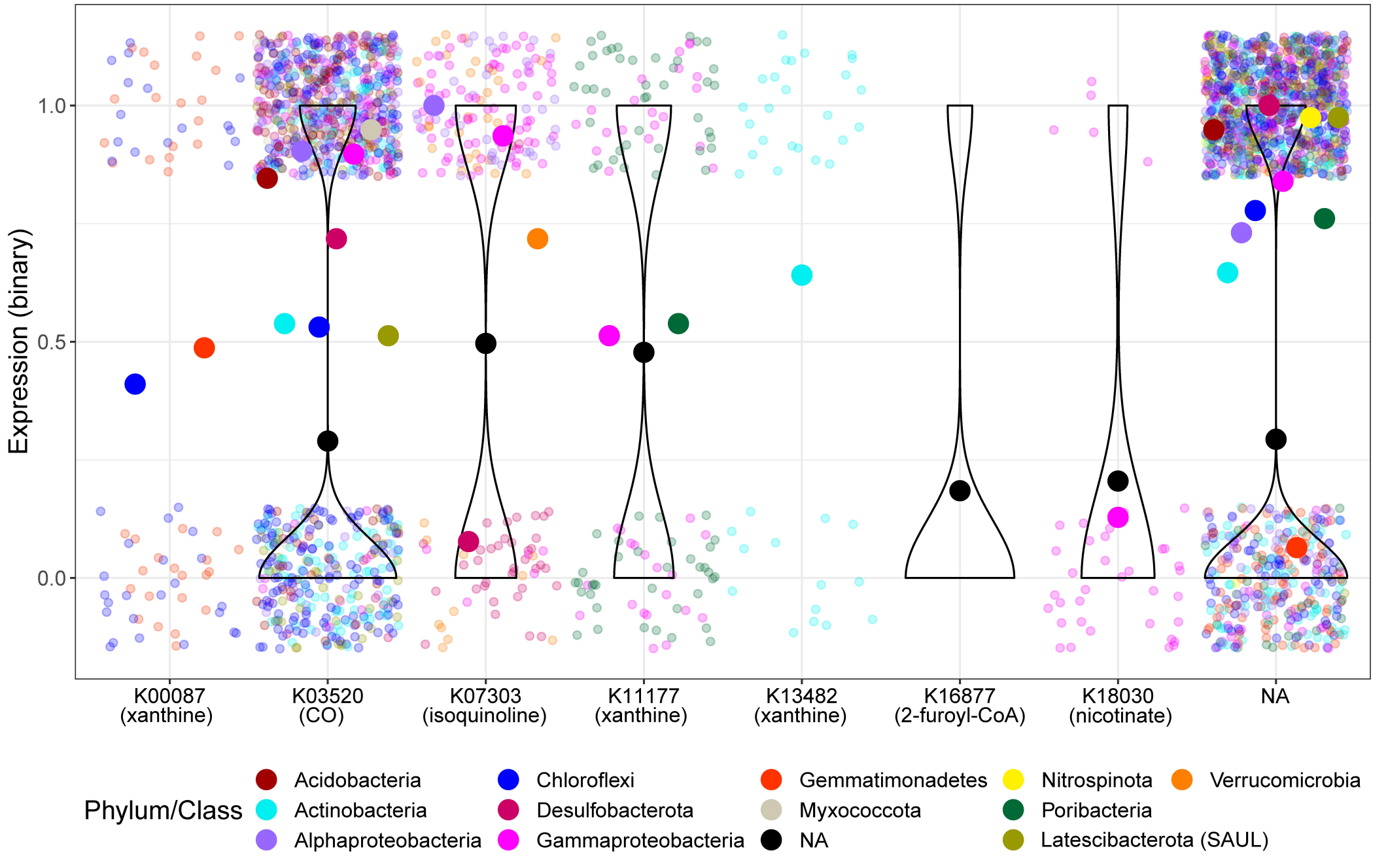
Expression (binary)
1.0
0.5
0.0
K00087 (xanthine)
K03520 (CO)
K07303 (isoquinoline)
K11177 (xanthine)
K13482 (xanthine)
K16877 (2-furoyl-CoA)
K18030 (nicotinate)
NA
Phylum/Class
Acidobacteria
Actinobacteria
Alphaproteobacteria
Chloroflexi
Desulfobacterota
Gammaproteobacteria
Gemmatimonadetes
Myxococcota
NA
Nitrospinota
Poribacteria
Latescibacterota (SAUL)
Verrucomicrobia

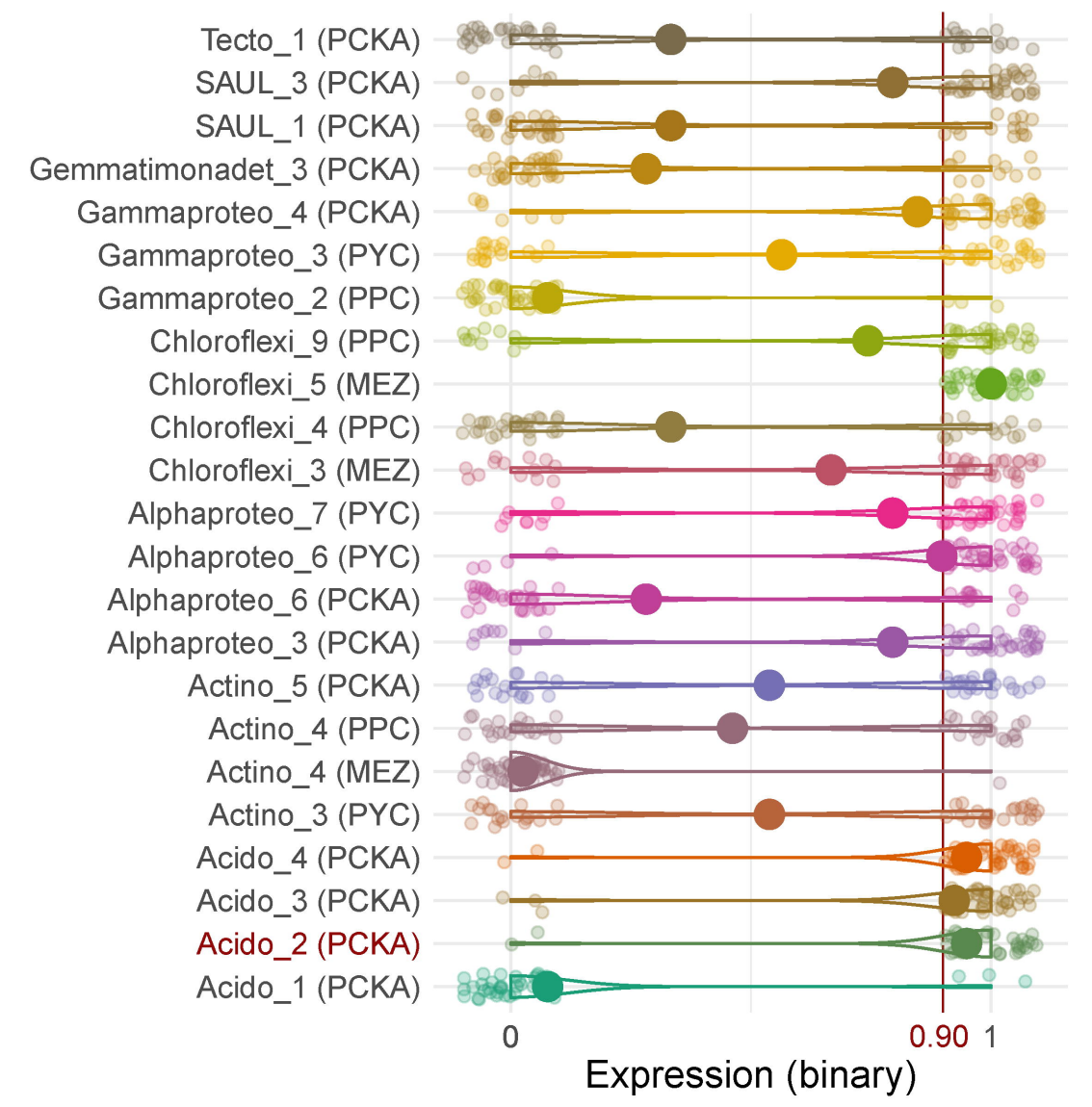
Tecto_1 (PCKA)
SAUL_3 (PCKA)
SAUL_1 (PCKA)
Gemmatimonadet_3 (PCKA)
Gammaproteo_4 (PCKA)
Gammaproteo_3 (PYC)
Gammaproteo_2 (PPC)
Chloroflexi_9 (PPC)
Chloroflexi_5 (MEZ)
Chloroflexi_4 (PPC)
Chloroflexi_3 (MEZ)
Alphaproteo_7 (PYC)
Alphaproteo_6 (PYC)
Alphaproteo_6 (PCKA)
Alphaproteo_3 (PCKA)
Actino_5 (PCKA)
Actino_4 (PPC)
Actino_4 (MEZ)
Actino_3 (PYC)
Acido_4 (PCKA)
Acido_3 (PCKA)
Acido_2 (PCKA)
Acido_1 (PCKA)
0
0.90
1
Expression (binary)